Molecules and Cells

Improving the Safety of Mesenchymal Stem Cell-Based *Ex Vivo* Therapy Using Herpes Simplex Virus Thymidine Kinase

Narayan Bashyal[1,2,5], Tae-Young Lee[3,5], Da-Young Chang[3], Jin-Hwa Jung[1], Min Gyeong Kim[1,2], Rakshya Acharya[1], Sung-Soo Kim[1,2], Il-Hoan Oh[4,*], and Haeyoung Suh-Kim[1,2,3,*]

[1]Department of Anatomy, Ajou University School of Medicine, Suwon 16499, Korea, [2]Department of Biomedical Sciences, Graduate School, Ajou University School of Medicine, Suwon 16499, Korea, [3]Research Center, Cell&Brain Co., Ltd., Jeonju 54871, Korea, [4]Department of Medical Lifescience, The Catholic University of Korea, College of Medicine, Seoul 06591, Korea, [5]These authors contributed equally to this work.
*Correspondence: iho@catholic.ac.kr (IHO); hysuh@ajou.ac.kr (HSK)
https://doi.org/10.14348/molcells.2022.5015
www.molcells.org

Human mesenchymal stem cells (MSCs) are multipotent stem cells that have been intensively studied as therapeutic tools for a variety of disorders. To enhance the efficacy of MSCs, therapeutic genes are introduced using retroviral and lentiviral vectors. However, serious adverse events (SAEs) such as tumorigenesis can be induced by insertional mutagenesis. We generated lentiviral vectors encoding the wild-type herpes simplex virus thymidine kinase (HSV-TK) gene and a gene containing a point mutation that results in an alanine to histidine substitution at residue 168 (TK(A168H)) and transduced expression in MSCs (MSC-TK and MSC-TK(A168H)). Transduction of lentiviral vectors encoding the TK(A168H) mutant did not alter the proliferation capacity, mesodermal differentiation potential, or surface antigenicity of MSCs. The MSC-TK(A168H) cells were genetically stable, as shown by karyotyping. MSC-TK(A168H) responded to ganciclovir (GCV) with an half maximal inhibitory concentration (IC_{50}) value 10-fold less than that of MSC-TK. Because MSC-TK(A168H) cells were found to be non-tumorigenic, a U87-TK(A168H) subcutaneous tumor was used as a SAE-like condition and we evaluated the effect of valganciclovir (vGCV), an oral prodrug for GCV. U87-TK(A168H) tumors were more efficiently ablated by 200 mg/kg vGCV than U87-TK tumors. These results indicate that MSC-TK(A168H) cells appear to be pre-clinically safe for therapeutic use. We propose that genetic modification with HSV-TK(A168H) makes allogeneic MSC-based *ex vivo* therapy safer by eliminating transplanted cells during SAEs such as uncontrolled cell proliferation.

Keywords: herpes simplex virus-thymidine kinase, lentiviral vector, mesenchymal stem cells, safety switch, stemness

INTRODUCTION

Mesenchymal stem cells (MSCs) are self-renewing multipotent stem cells capable of differentiating into mesodermal lineages, such as adipogenic, osteogenic, and chondrogenic cells (Pittenger et al., 1999). MSCs also have the potential to transdifferentiate into ectodermal lineages (neurons and keratinocytes) (Dos Santos et al., 2019; Poudineh et al., 2018) and endodermal lineages (hepatocytes and cardiomyocytes) (Aurich et al., 2009; Sgodda et al., 2007; Szaraz et al., 2017). In addition to their differentiation potential into multiple lineages, MSCs have been considered as a cell-based drug

Received 8 November, 2021; revised 26 November, 2021; accepted 16 December, 2021; published online 21 March, 2022

eISSN: 0219-1032
©The Korean Society for Molecular and Cellular Biology.
This is an open-access article distributed under the terms of the Creative Commons Attribution-NonCommercial-ShareAlike 3.0 Unported License. To view a copy of this license, visit http://creativecommons.org/licenses/by-nc-sa/3.0/.

to treat various neurological disorders, such as amyotrophic lateral sclerosis (Mazzini et al., 2003; Suzuki et al., 2008), Parkinson's disease (Kan et al., 2007; Wang et al., 2010), Alzheimer's disease (Ma et al., 2013; Yang et al., 2013), stroke (Lee et al., 2015; Xin et al., 2013), and non-neurological diseases, such as graft versus host diseases (Le Blanc et al., 2004), myocardial infraction (Huang et al., 2019), type 1 diabetes (Unsal et al., 2015) and severe asthma (Shin et al., 2021). More than 1,300 clinical trials are ongoing or have been completed worldwide using MSCs (https://www.clinicaltrials.gov, with a query of "mesenchymal stem cells" 2021), indicating the broad application and usefulness of naive MSCs in cell-based drug development.

Several genetic modification approaches have been applied to MSCs to enhance their therapeutic efficacy. Currently, viral vectors using adenoviruses, retroviruses, and lentiviruses are commonly used to transfer functional genes into MSCs, whereas transfection of non-viral vectors is inefficient (Kim et al., 2003; Park et al., 2015). Adenovirus vectors require high multiplicity of infection (MOI) for efficient transduction, which affects the growth kinetics and adipogenic differentiation of MSCs (Marasini et al., 2017).

In early studies, first-generation retrovirus encoding γc cDNA led to acute lymphoblastic leukemia in patients with X-linked severe combined immunodeficiency (SCID-X1) following infusion of transduced CD34+ hematopoietic stem cells. Extensive studies have shown that insertion of the retroviral long-term repeat (LTR) sequence leads to aberrant expression of oncogenes such as *LMO2* or *CCND2* (Hacein-Bey-Abina et al., 2014). In contrast, unlike hematopoietic stem cells, retroviruses efficiently transduce MSCs without interfering with growth kinetics and stemness or inducing tumorigenicity (Park et al., 2013). Meanwhile, a third-generation lentivirus with self-inactivating (SIN) LTRs has been developed to reduce the risk of insertional mutagenesis without sacrificing transduction efficiency (De Ravin et al., 2016; Hetzel et al., 2017). Phase I and Phase II clinical trials with lentivirus did not show any adverse events 8 years after virus injection (McGarrity et al., 2013), although there is a theoretical probability of insertional oncogenesis. However, although several studies have investigated lentiviral transduction in MSCs, the maintenance of stem cell properties after lentivirus transduction has not been sufficiently investigated (Lin et al., 2012).

The chromosomal integration of retroviral and lentiviral vectors allows for sustained gene expression but can be a double-edged sword—it can also cause serious side effects, such as uncontrolled cell growth by activating nearby oncogenes. To mitigate such possible risks, suicide genes such as herpes simplex virus thymidine kinase I (HSV-TK) and inducible caspase-9 have been included in viral vectors (Greco et al., 2015; Ramos et al., 2010). HSV-TK phosphorylates anti-viral agents such as ganciclovir (GCV) or acyclovir (ACV), thereby inducing the incorporation of GCV- or ACV-derivatives into nascent DNA, leading to cell death by apoptosis (Beltinger et al., 1999; Field et al., 1983; Reardon, 1989; Zhang et al., 2008). Previously, we developed MSCs to carry the cytosine deaminase gene for the therapy of brain tumor. CD exerts converts 5-fluorocytosine (a prodrug) to 5-fluorouracil (an anti-cancer drug) and eliminates neighboring cancer cells (Chang et al., 2010). In contrast to CD gene, the cytotoxic effect of HSV-TK is minimal to neighboring cells unless the cells communicate via gap junctions because GCV- or ACV-derivatives are not membrane-permeable. Therefore, HSV-TK may provide a better tool as a safety gene to abolish unwanted serious adverse events (SAEs) by inducing apoptosis of transplanted cells. Several TK mutants have been tested to reduce the binding competition of thymidine to GCV. In particular, TK(A168H), which contains a mutation resulting in a substitution of alanine to histidine at residue 168, has 4-fold higher GCV kinase activity than wild-type (WT) TK (Balzarini et al., 2006), thereby lowering the burden of using high-dose GCV in the clinical field. Thus, we hypothesized that the TK(A168H) mutant might function better than TK as a safety switch.

In this study, we engineered bone marrow-derived MSCs to express TK(A168H) using lentiviral vectors. We tested the stem cell characteristics, genetic stability, and tumorigenic potential of transduced MSCs. To explore the safety switch functions of TK(A168H), we compared the cytotoxic effects of TK and TK(A168H) in response to GCV. Because MSCs expressing TK(A168H) were not tumorigenic, we utilized the glioma cell line U87 expressing TK(A168H) to establish *in vivo* tumor models and tested whether the U87-TK(A168H) cells could be eliminated by GCV treatment. We show that lentivirus carrying TK(A168H) can be utilized to deliver therapeutic genes without affecting the stem cell properties of MSCs and to provide a safety switch which can be turned on by administration of the anti-viral drug GCV in the case of SAEs.

MATERIALS AND METHODS

Animals

All experimental procedures using animals were approved by the Institutional Animal Care and Use Committee (IACUC) of Ajou University School of Medicine, South Korea (No. 2020-0009). Immune-compromised mice such as NSG mice (NOD.Cg-*Prkdc*^{scid}*Il2rg*^{tm1Wjl}/SzJ, Cat. No. 005557; The Jackson Laboratory, USA) and nude mice (Hsd: Athymic Nude-Foxn1^{nu}; Envigo, USA) were used to make tumor models. The mice were housed with ad libitum access to food and water and maintained in a 12:12 h light-dark cycle until being euthanized.

Human MSCs isolation and culture

Human MSCs were purified from bone marrow aspirated from the iliac crest of a 19-year-old healthy donor for allogeneic transplantation. The MSCs were isolated as described previously (Kim et al., 2005) with approval from the Institutional Review Board of Ajou University Medical Center (No. AJIRB-BMR-KSP-20-040) with the informed consent of the patient. Briefly, mononucleate cells were collected and maintained as adherent cultures in Dulbecco's Modified Eagle's Medium (DMEM, Cat. No. LM 001-05; Welgene, Korea) supplemented with 10% fetal bovine serum (FBS, Cat. No. 16000-044; Gibco, USA), 100 U/ml penicillin, 100 μg/ml streptomycin (Cat. No. 15140-122; Gibco) and 10 ng/ml basic fibroblast growth factor (Cat. No. 100-18B; PeproTech, USA).

Lentiviral vectors and cell lines

WT TK cDNA was polymerase chain reaction (PCR) amplified from pAL119- TK (Cat. No. 21911; Addgene, USA) using a forward (5'-ACCGGTGCCACCATGGCTTCGTACCCCT-GC-3') and a reverse primer (5'-ACCGGTCTCAGTTAGCCTC-CCCCATC-3'). The product was subcloned into the pGEM-T-easy vector. To generate the TK(A168H) mutant, site-directed mutagenesis was carried out using a mutant forward primer (5'-CGCCATCCCATCGCCCACCTCCTGTGCTAC-3') and mutant reverse primer (5'-GTAGCACAGGAGGTGGGCGATGGGAT-GGCG-3') paired with the primers that were used to obtain TK cDNA. The mutant PCR product was also subcloned into the pGEM-T-easy vector. The puromycin resistance gene that is situated between the SV40 promoter and Woodchuck Hepatitis Virus (WHV) Posttranscriptional Regulatory Element (WPRE) in the pLenti-Bicistronic plasmid (Cat. No. LV037; Applied Biological Materials [ABM], Canada) was replaced by TK and TK(A168H) cDNAs through a serial process of enzyme digestion and ligation. CopGFP cDNA was inserted into multiple cloning sites in the pLenti-Bicistronic plasmid from pLenti-GIII-CMV-GFP-2A-Puro (Cat. No. LV180162; ABM) to obtain pLenti-TK and pLenti-TK(A168H). As a result, TK gene expression was driven by the SV40 promoter and CopGFP expression was driven by the PGK promoter in our lentiviral transfer plasmids. These transfer plasmids were packaged into lentiviral vectors, Lenti-TK and Lenti-TK(A168H), in the Lenti-X™ 293T(293T-X) cell line (Cat. No. 632180; TaKaRa, USA), following a previously described method (Lee et al., 2020).

U87 cells and MSCs were transduced with Lenti-TK and Lenti-TK(A168H) virus for 8 h in the presence of 4 μg/ml polybrene to obtain U87-TK, U87-TK(A168H), MSC-TK, and MSC-TK(A168H) cell lines. U87/GFP without the TK gene was generated by transducing U87 cells with a pLL3.7-drived lentiviral vector (Park et al., 2013). All U87 cell lines were selected for CopGFP expression by fluorescence-activated cell sorting (FACS) after transduction, as described previously (Chang et al., 2020).

FACS

Briefly, U87-TK, U87-TK(A168H), MSC-TK, and MSC-TK(A168H) cells were harvested using 0.25% trypsin-EDTA (Cat. No. 25200056; Thermo Fisher Scientific, USA). After washing with phosphate-buffered saline (PBS), the cells were resuspended in eBioscience™ Flow Cytometry Staining Buffer (Cat. No. 00422226; Invitrogen, USA). GFP-positive cells were sorted using an Attune NxT Acoustic Focusing Cytometer (Invitrogen) with Attune™ NxT software. The percentage of GFP-positive cells was determined by FACS analysis.

Surface antigen analysis

To measure the expression of surface antigens in MSC-TK(A168H) or MSCs, FACS analysis was performed as described previously (Park et al., 2013). Briefly, cells were stained for 15 min at 25℃ with fluorochrome-conjugated antibodies against CD29 (Cat. No. 303003; BioLegend, USA), CD90 (Cat. No. 559869; BD Biosciences, USA), CD105 (Cat. No. 323205; BioLegend), CD34 (Cat. No. 343505; BioLegend), CD45 (Cat. No. 304011; BioLegend), HLA-DR (Cat. No. 560896; BD Pharmingen™, USA), and isotype control. The cells were washed with PBS and suspended in flow cytometry staining buffer. Cells were analyzed using an Attune NxT Acoustic Focusing Cytometer (Thermo Fisher Scientific) with Attune™ NxT software.

Western blot

When the cells were grown to confluence in 100 mm dishes, they were lysed in RIPA lysis and extraction buffer (Cat. No. 89901; Thermo Fisher Scientific) containing a protease inhibitor cocktail (P2714; Sigma-Aldrich, USA). After centrifugation at 12,000 × *g* at 4°C, the supernatant was collected. Protein concentration was determined using the Pierce™ bicinchoninic acid (BCA) Protein Assay Kit (Cat. No. 23225; Thermo Fisher Scientific) and 20 μg of protein for each sample was separated by sodium dodecyl sulfate polyacrylamide gel electrophoresis (SDS-PAGE). The proteins were transferred to a polyvinylidene fluoride (PVDF) membrane (Cat. No.1060021; GE Healthcare, USA) and visualized using SuperSignal™ West Pico PLUS Chemiluminescent Substrate, as recommended by the manufacturer. Primary antibodies were used for HSV-TK (1:1,000 dilution, LSC415730; LSBio, USA) and glyceraldehyde-3-phosphate dehydrogenase (GAPDH) (1:1,000 dilution, Cat. No. sc-32233; Santa Cruz Biotechnology, USA). The secondary antibodies were horseradish peroxidase-conjugated anti-mouse or anti-rabbit IgG (Cat. No. A9044 [Sigma-Aldrich] or Cat. No. G-21234 [Thermo Fisher Scientific], respectively).

Mesodermal differentiation assay

Naïve MSC and MSC-TK(A168H) cells were plated at a density of 5×10^4 in a 24-well plate and allowed to grow to confluence. Adipogenic and osteogenic differentiations were carried out by replacing the media every 2-3 days in StemPro™ osteogenesis differentiation media (Cat. No. A1007201; Thermo Fisher Scientific) and StemPro™ adipogenesis differentiation media (Cat. No. A1007001; Thermo Fisher Scientific). After 14 days, the differentiated cells were washed with PBS and fixed with 10% neutral buffered formalin (Cat. No. 015MIRA01; BBC Biochemical, USA). For adipogenesis, oil-red O staining was carried out and the number of oil-red O positive adipocytes was counted from 64 images taken from four independent samples under 10× magnification using Image Express Micro4 (Molecular Devices, USA). For osteogenesis, alizarin red S staining was performed, and at least 10 random images were taken from four independent samples using an EVOS M5000 imaging system (Thermo Fisher Scientific), and the positive area was measured semi-manually by excluding negative areas with the help of color thresholding from ImageJ software (ver. 1.53e; NIH, USA). For chondrogenesis, 3×10^5 cells were washed with PBS and centrifuged at 500 × *g* for 5 min. The cell pellet was induced for chondrogenic differentiation in StemPro™ chondrogenesis differentiation media (Cat. No. A1007101; Thermo Fisher Scientific) for 4 weeks by replacing the media every 2-3 days. After completion of chondrogenic induction, the pellets were washed with PBS and the three-dimensional images were taken with an OLYMPUS U-RFL-T microscope (Olympus, Japan). The pellet diameter was calculated using ImageJ software, and the pellet surface area (SA) was estimated using the formula

SA = $4\pi \cdot r^2$. The pellets were fixed in 10% neutral buffered formalin for 30 min at room temperature, washed, and embedded in paraffin. Chondrogenic pellets were sectioned at a thickness of 5 μm, and at least three serial mid-sections were deparaffinized and stained with Alcian blue solution for 1 h at room temperature. After counterstaining with nuclear red for 3 min at room temperature, the samples were mounted using Shandon Synthetic Mountant™ (Cat. No. 6769007; Thermo Fisher Scientific). The stained images were acquired using an EVOS M5000 imaging system and converted into 8-bit images. The Alcian blue-positive area was measured semi-manually by excluding the negative area from the total chondrogenic pellet area with the help of thresholding using ImageJ software.

Growth kinetic assay

MSCs and MSC-TK(A168H) cells were maintained by subculturing every 6-8 days in the growth media as mentioned above for human MSC isolation and culture methods. To compare the growth kinetics of MSCs with MSC-TK(A168H) cells, cells were stained with trypan blue and live cells in 0.4 μl of Countess® Cell Counting Chamber Slides were counted in duplicates per chamber (Thermo Fisher Scientific) at confluency and plated at a density of 1,000 cells/cm^2 for the next passage in culture. Cell counts in two chambers were used to extrapolate cumulative cell numbers. All cell culture media were replaced with fresh media every 2-3 days. Cell population doubling time was calculated as previously described (Rothenburger et al., 2021).

Quantitative reverse transcription (qRT)-PCR

Total RNA was extracted from the cells at confluence, and PCR was performed as described previously (Lee et al., 2020). Forward and reverse primers were used to amplify TK, connexin 40 (Cx40), Cx43, and Cx45. Expression of Human GAPDH was used to normalize RNA expression. The primer sequences used for qRT-PCR are listed in Table 1.

Chromosomal stability

Karyotyping analysis was carried out in MSCs and MSC-TK(A168H) on passage 7 (P7) and P10 as described previously (Park et al., 2013) using CytoVision (Applied Imaging International, USA) at the Clinical Cytogenetics Laboratory at Ajou University Hospital (http://www.ajoumc.or.kr).

In vitro suicide effect of HSV-TK

MSC-TK and MSC-TK(A168H) cells were seeded at a density of 2 × 10^3 cells/well, while U87-TK and U87-TK(A168H) cells were seeded at 1 × 10^4 cells/well in 12-well plates. After 24 h of incubation, cells were treated with GCV (Cat. No. G2536; Sigma-Aldrich), at the indicated concentrations. In MSCs, the media was replaced every two days with fresh growth media containing the indicated concentrations of GCV. On 6th day, 3-[4,5-dimethyl-thiazol-2-yl]-2, 5-diphenyltetrazolium bromide (MTT) was added to a final concentration of 0.5 mg/ml (Cat. No. M2128; Sigma-Aldrich). U87-driven cells were cultured as described above, except that the medium was not changed for the 4 days until MTT was added to the culture. After 2 h incubation, the MTT-formazan product was extracted in 500 μl/well dimethyl sulfoxide (DMSO) and the absorbance at 540 nm was measured. The viability of the treated cells was expressed relative to that of the untreated control cells as the mean ± SEM of eight and five independent experiments for MSC and U87 driven cells respectively.

Tumorigenicity assay of lentiviral transduced MSCs

To carry out the *in vivo* tumorigenicity assay, 10^6 MSCs and MSC-TK(A168H) cells were suspended in 100 μl of PBS containing 20% Corning® Matrigel® Growth Factor Reduced (GFR) Basement Membrane Matrix, LDEV-free (Cat. No.354230; Corning, USA) and subsequently inoculated subcutaneously into NSG mice.

In vivo suicide effect of HSV-TK

To mimic a SAE, 10^6 each of U87-TK and U87-TK(A168H) cells in 100 μL of PBS containing 20% Corning® Matrigel® Growth Factor Reduced (GFR) Basement Membrane Matrix, LDEV-free (Cat. No. 354230; Corning) were injected subcutaneously into 6-week-old NSG or nude mice. After the tumor size reached approximately 100-300 mm^3, the animals orally received 50, 200, 400, or 800 mg/kg of valganciclovir (vGCV, Cat. No. V0158; Tokyo Chemical Industry, Japan) dissolved in normal saline once daily for 14 days. Tumor dimensions were measured every 2 days with a caliper, and the volumes were calculated using the following formula: Volume = $\pi/6$ × length × width × height (Tomayko and Reynolds, 1989). U87-GFP cells were used in a similar manner to serve as a negative control.

Statistical analysis

Statistical analyses were performed SigmaPlot™ v14 software (Systat Software, USA). Data were analyzed using the Student's *t*-test or one-way ANOVA. Significant differences were further evaluated using Student–Newman–Keuls test. *P* values < 0.05 was considered statistically significant. All data are expressed as the mean ± SEM.

Table 1. qRT-PCR primer list

Gene	Forward primer sequence 5'-3'	Reverse primer sequence 5'-3'
HSV-TK	GGAGGACAGACACATCGACC	TATTGGCAAGCAGCCCGTAA
Cx40	CCTCTTCATATTCCGTATGCT	GTGGAGACGAAGATGATCTG
Cx43	CACATCAGGTGGACTGTTTCCTCT	TTAACCCGATCCTTAACGCCCTTG
Cx45	GAGCTTCCTGACTCGCCTGCT	CCCGGCTGTTCTGTGTTGCAC
GAPDH	GTCTCCTCTGACTTCAACAGC	ACCACCCTGTTGCTGTAGCCAA

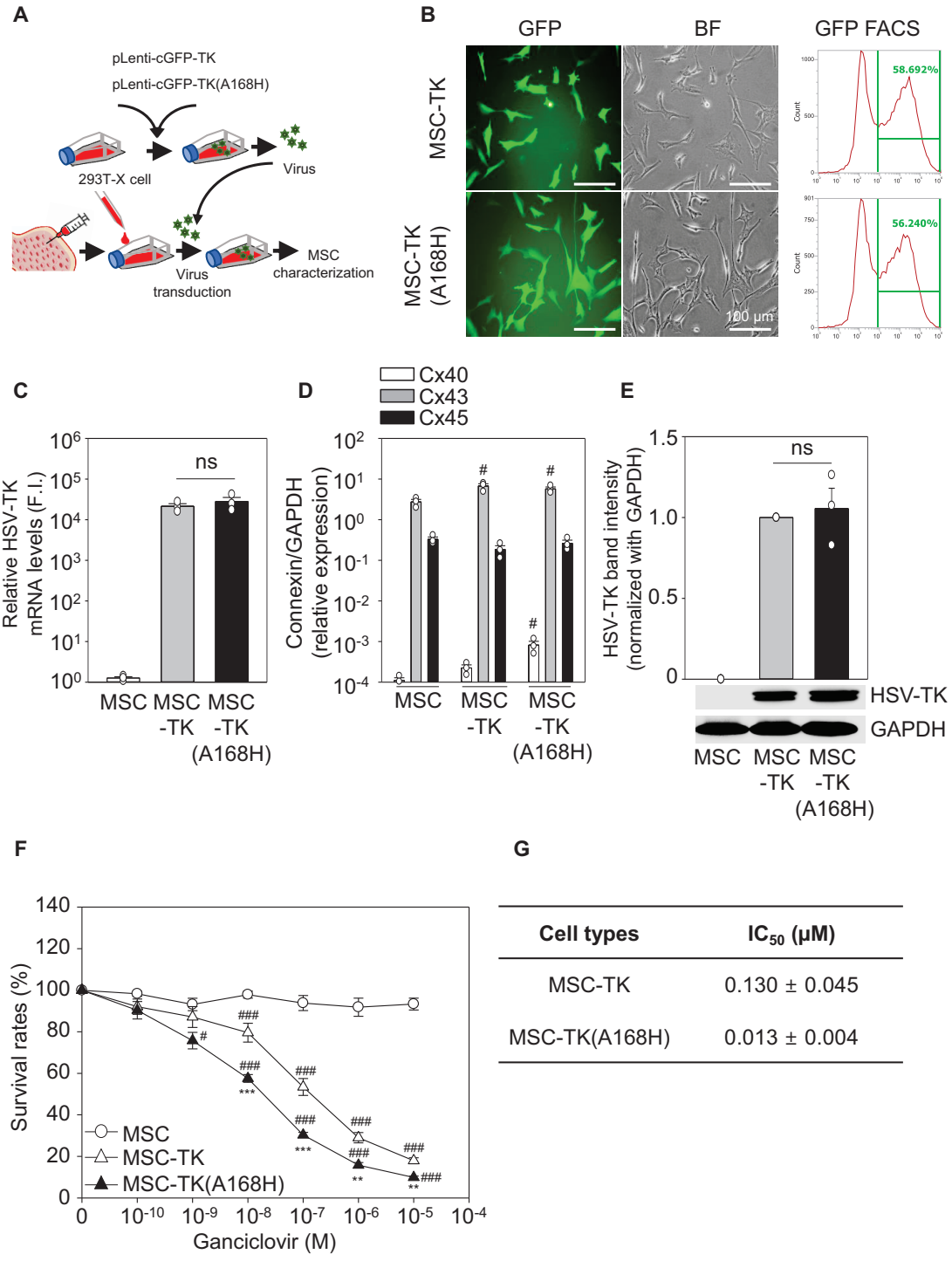

Cell types	IC_{50} (μM)
MSC-TK	0.130 ± 0.045
MSC-TK(A168H)	0.013 ± 0.004

Fig. 1. Cytotoxic effects of HSV-TK and GCV in MSCs expressing TK and TK(A168H). (A) Schematic presentation showing the method to generate TK-expressing MSCs. Lentivirus carrying CopGFP and WT HSV-TK or HSV-TK(A168H) were packaged in 293T-X cells. (B) Representative fluorescence images of lentivirus-transduced MSC-TK (WT) and MSC-TK(A168H) and their FACS analysis showing the copGFP-positive cells and transduction efficiency. (C) RT-qPCR analysis indicating similar level of relative TK gene expression as fold induction (F.I.) with respect to the naïve MSC mRNA level in MSC-TK and MSC-TK(A168H). (D) RT-qPCR analysis showing higher CX43 expression in TK expressing MSC compared to naïve MSCs, comparable amounts of Cx45, but minimal levels of Cx40. (E) Western blot analysis showing relative levels of TK protein expression in transduced cells. GAPDH was used as a loading control. (F) MTT assay indicating the cytotoxic effect of GCV on MSC-TK and MSC-TK(A168H). (G) IC_{50} values for GCV in MSC-TK and MSC-TK(A168H). Data are mean ± SEM of three independent experiments ($^{\#}P < 0.05$, $^{\#\#\#}P < 0.001$ compared to MSC and $^{**}P < 0.01$, $^{***}P < 0.001$, compared to MSC-TK in; one-way ANOVA test). ns, not significant.

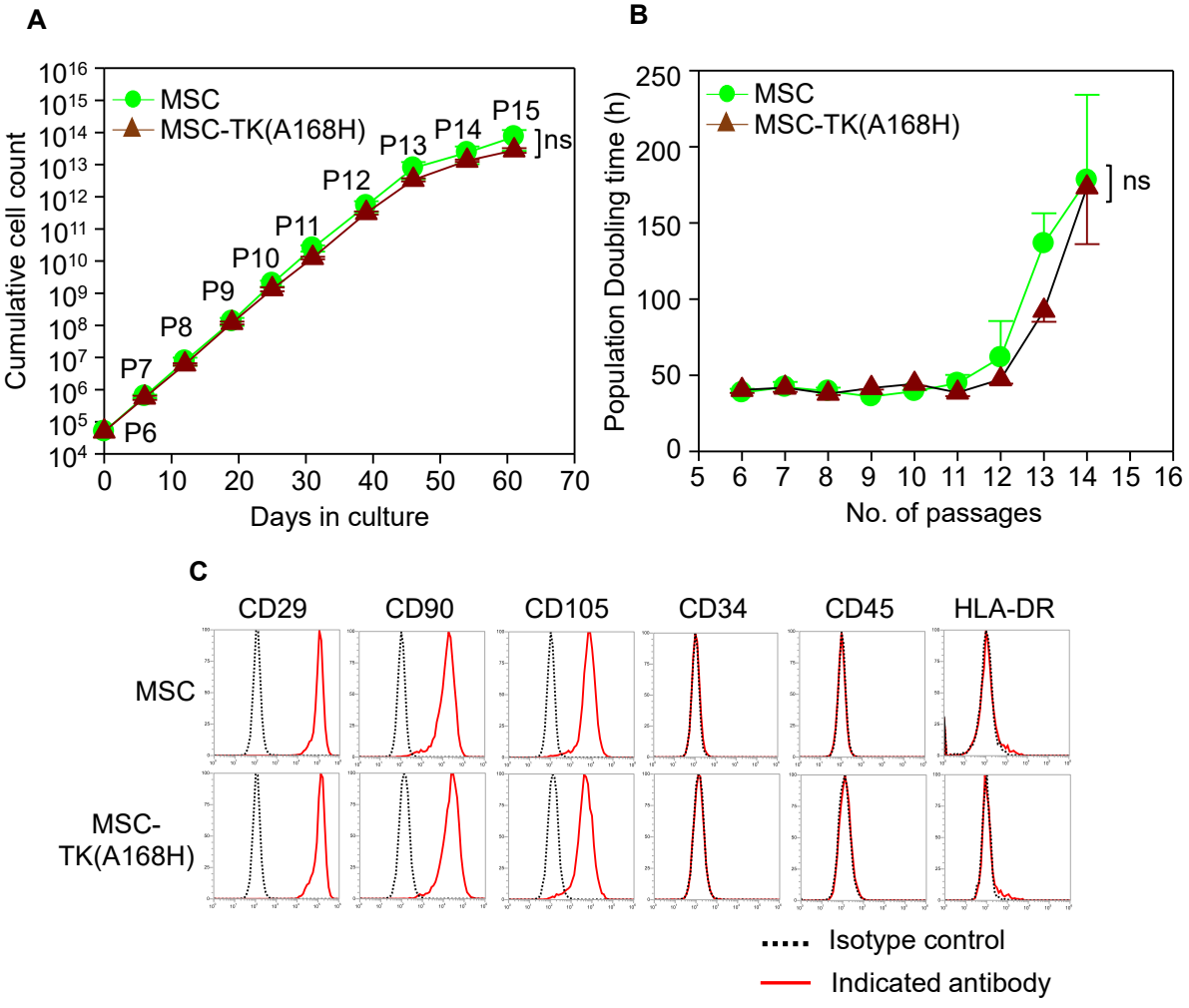

D

Marker	MSC	MSC-TK(A168H)
CD29	99.84 ± 0.03	99.57 ± 0.18
CD90	97.91 ± 0.64	95.98 ± 1.33
CD105	95.51 ± 2.05	95.86 ± 0.56
CD34	0.40 ± 0.23	0.18 ± 0.03
CD45	0.10 ± 0.03	0.21 ± 0.10
HLA-DR	0.71 ± 0.05	0.71 ± 0.21

Fig. 2. Stem properties are not altered by overexpression of TK(A168H) in MSC. (A) MSCs were transduced at P5 and subcultured until P15. When the culture reached to confluency, the number of cells were counted and used for growth kinetics. Data are mean ± SEM from 2-3 independent experiments, each performed in duplicates. (B) Population doubling time of MSC, and MSC-TK(A168H) cells were determined from P6 to P14. Data are mean ± SEM from 2-3 independent experiments, each performed in duplicates. (C) FACS analysis showing the surface antigen expression in MSCs and MSC-TK(A168H) cells. Isotype controls were used to determine the backgrounds. (D) Summary of FACS analysis showing the similar phenotype of MSCs and MSC-TK(A168H): positive for CD29, CD90, and CD105 and negative for CD34, CD45, and HLA-DR. Black dotted peaks indicate the results obtained from cells stained with isotype control antibodies and red peaks indicate the results of cells stained with the indicated specific target antibodies. Data are mean ± SEM from 3 independent experiments. ns, not significant in each passage compared to MSC.

RESULTS

Generation of HSV-TK expressing MSCs

Plasmids encoding TK and TK(A168H) were packaged into lentiviral vectors in 293T-X cells and transduced into MSCs to obtain MSC-TK and MSC-TK(A168H) cells (Fig. 1A). FACS analysis indicated that copGFP was detected in 58% of MSC-TK and 56% of MSC-TK(A168H) cells (Fig. 1B). RT-PCR and western blot analyses showed similar levels of HSV-TK expression in MSC-TK and MSC-TK(A168H) cells (Figs. 1C and 1E). To address the gap junction-mediated bystander effect in TK-expressing MSCs, expression of the major components of gap junctions, such as Cx43, Cx40, and Cx45, were confirmed in MSCs, MSC-TK, and MSC-TK(A168H) cells. These cell lines expressed high levels of Cx43 and Cx45, but minimally expressed Cx40 (Fig. 1D). Expression of Cx43 was significantly higher in MSC-TK and MSC-TK(A168H) compared to MSCs. Cx40 gene expression was increased in MSC-TK(A168H) whereas Cx45 expression was similar in all cell lines. To compare the viabilities of cells expressing TK and TK(A168H), an MTT assay was carried out using MSC-TK and MSC-TK (A168H) cells. GCV was dissolved in DMSO and added to the culture to a final concentration of 10 μM. GCV inhibited cell growth for 6 days and half maximal inhibitory concentration (IC_{50}) values, the concentration required to kill 50% of cells, were 0.130 ± 0.045 μM and 0.013 ± 0.004 μM for MSC-TK and MSC-TK(A168H) cells, respectively (Figs. 1F and 1G). The MSC-TK(A168H) IC_{50} value was 10-fold lower than that of MSC-TK cells. We found that the TK(A168H) substitution did not alter transcription or translation of the TK gene (Figs. 1C and 1E). Higher concentrations of GCV interfered with cell growth regardless of the status of HSV-TK, likely because of the high concentration of DMSO (data not shown). The results show that the cell lines expressed TK and TK(A168H) to a similar level. Thus, the approximately 10-fold higher responsiveness and lower IC_{50} value of MSC-TK(A168H) should be a result of the altered enzyme activity of TK(A168H) compared to TK. We focused on TK(A168H) as a safety switch in subsequent studies.

Stem cell properties of MSC-TK(A168H)

We characterized the cells to determine whether lentiviral transduction altered the stem cell-like properties of MSCs. MSCs and MSC-TK(A168H) cells were plated at a density of 5×10^4 cells per 100 mm dish and subcultured at the same density until P15, when the cells stopped growing. MSCs and MSC-TK(A168H) cells exponentially expanded by approximately 9- to 14-fold per subculturing every 6 days until P12 (Fig. 2A), after which the doubling time was dramatically increased (Fig. 2B). FACS analysis indicated that surface antigens including CD29, CD90, CD105 (positive), CD34, CD45, and HLA-DR (negative) were similar in both cell lines (Figs. 2C and 2D). The indistinguishable growth rates and surface antigenicity between both cell lines indicate that lentiviral transduction does not alter the growth kinetics or surface antigenic properties.

Next, we tested the differentiation potential of MSCs and MSC-TK(A168H) cells into mesodermal lineage cells. Both MSCs and MSC-TK(A168H) cells formed chondrogenic pellets (Fig. 3A). Like MSCs, copGFP-positive MSC-TK(A168H) cells secreted an Alcian blue-positive extracellular matrix (white arrow in Fig. 3A). Likewise, copGFP-positive MSC-TK(A168H) cells underwent adipogenic differentiation, as shown by oil red-positive lipid droplets (white arrow in Fig. 3B), and osteogenic differentiation, as shown by alizarin red-positive calcium deposition (white arrow in Fig. 3C). Quantitative analysis showed that the chondrogenic pellet SA and Alcian blue-positive area, the number of oil red-positive adipocytes, and the percentage of alizarin positive areas were similar between MSC-TK and MSC-TK(A168H) cells (Figs. 3D-3G). These findings suggest that HSV-TK(A168H)-expressing MSCs preserve their multilineage differentiation potential.

Genomic stability and tumorigenesis test of MSC-TK(A168H)

Although lentiviral vectors are known to be safe, chromosomal integration may induce tumorigenesis. We assessed the genomic stability of MSC-TK(A168H) cells in long-term culture using karyotyping analysis. MSC-TK(A168H) showed normal 46XY, as did naïve MSCs, at P7 and P10 (Figs. 4A and 4B, Supplementary Fig. S1). To assess tumorigenesis, we injected 10^6 MSCs and MSC-TK(A168H) cells, as well as U87 cells as a positive control, subcutaneously into NSG mice and monitored tumor formation. In the U87 injected group, the tumor was palpable 21 days after cell injection and reached a size of 5435.9 ± 375.8 mm^3 (Figs. 4E and 4F). In contrast, tumor-like structures were absent in the MSC and MSC-TK(A168H) groups up to 180 days, when the experiment was concluded (Figs. 4C and 4D). These findings clearly suggest that MSCs transduced with Lenti-TK(A168H) vectors are genetically safe.

Generation of U87-TK(A168H)

Because MSC-TK(A168H) cells are not tumorigenic, it is impossible to assess the functions of HSV-TK/GCV as a safety switch in the context of SAEs such as uncontrolled growth *in vivo*. Therefore, we established a U87-derived tumor model to mimic the SAE conditions. We generated U87-TK and U87-TK(A168H) cell lines using the same lentiviral vectors. The percentage of copGFP-expressing cells in U87-TK and U87-TK(A168H) cells was similar (Fig. 5A). RT-qPCR and western blot analyses indicated similar levels of TK mRNA and protein (Figs. 5B and 5D). Expression of gap junction components, such as Cx43, Cx40, and Cx45, were tested by RT-qPCR with U87s, U87-TK, and U87-TK(A168H) cells. These cell lines expressed high levels of Cx43 and Cx45, but minimally expressed Cx40 (Fig. 5C). The MTT assay was carried out in U87-TK and U87-TK (A168H) cells with escalating doses of GCV. The IC_{50} values were 0.213 ± 0.088 μM and 0.061 ± 0.012 μM for U87-TK and U87-TK(A168H) cells, respectively (Figs. 5E and 5F). The IC_{50} value was 3.5-fold lower in U87-TK(A168H) cells than in U87-TK cells. Consistent with MSC-driven cells, the GCV sensitivity of the TK(A168H) mutant was higher than that of TK in tumorigenic cells.

Effect of vGCV on U87-TK(A168H) tumor as a SAE model

Finally, we tested the usefulness of TK(A168H) as a safety switch in an *in vivo* tumor model. The effective dose of vGCV,

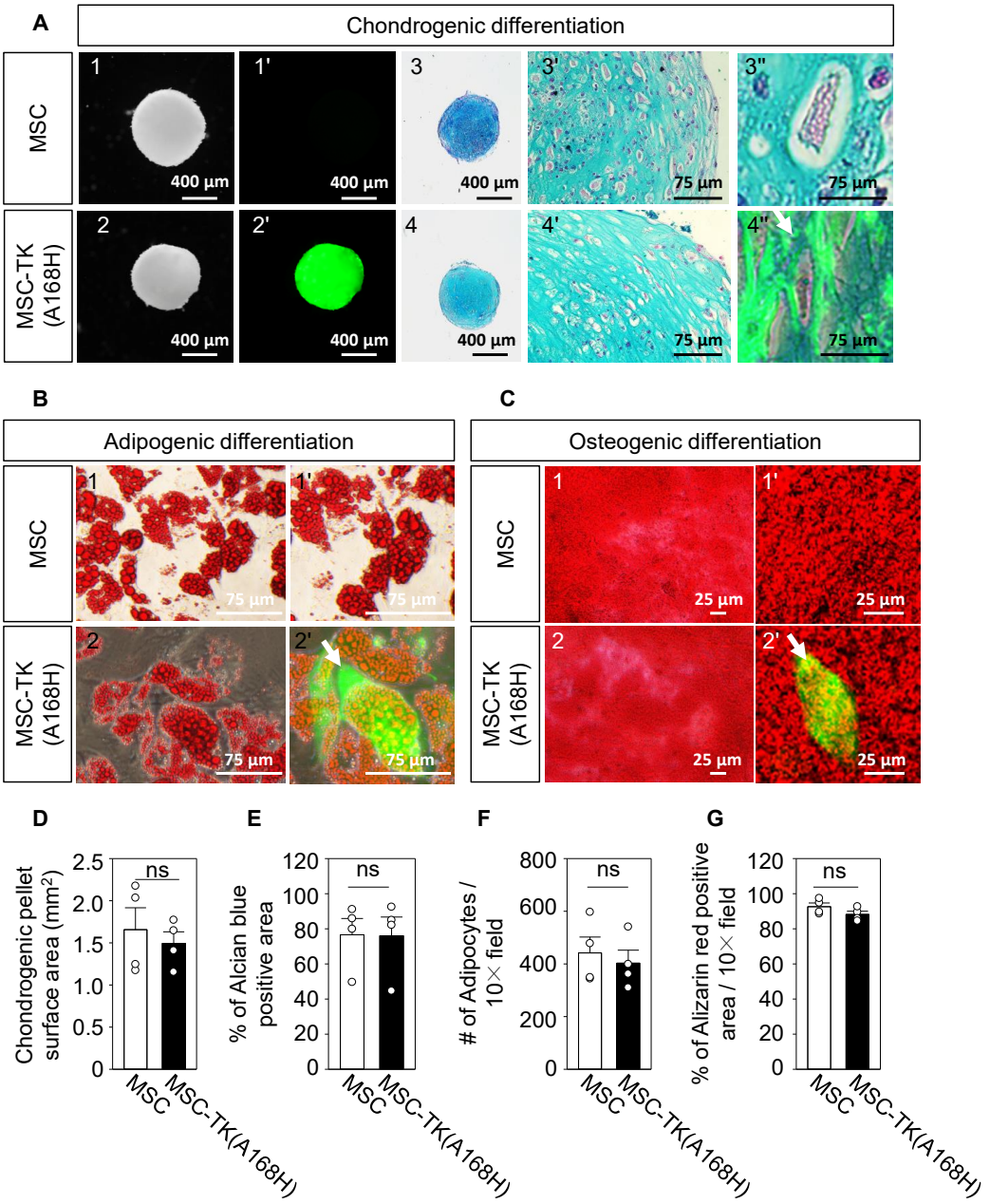

Fig. 3. Comparison of mesodermal differentiation potential of MSCs and MSC-TK(A168H). (A) Chondrogenic differentiation of MSC and MSC-TK(A168H) cells showing bright field (A1, A2), fluorescence (A1′, A2′), and Alcian blue staining (A3, A4) of the pellets. Higher magnification showing the Alcian blue-positive extracellular matrix secreted by chondrocytes in the lacuna (A3′, A4′). Note the copGFP in the cells and matrix (arrow in A4′′). (B) Adipogenic differentiation showing oil-red positive lipid droplets in MSCs and MSC-TK(A168H) cells in bright field microscopy (B1, B2) and fluorescence images (B1′, B2′). Note the oil red-positive copGFP expressing cell in fluorescence image (arrow in B2′). (C) Osteogenic differentiation showing alizarin red stained precipitates in bright field images of MSCs and MSC-TK(A168H) cells (C1 and C2). Note the alizarin red-positive copGFP expressing cell in fluorescence image (arrow in C2′). (D) Quantitative summary of chondrogenic differentiation of MSCs and MSC-TK(A168H) cells showing the chondrogenic pellet SA calculated from four independent experiments using ImageJ software. (E) Quantitative summary of Alcian blue-positive area was calculated from at least three mid-sagittal sections per pellet. Negative area was measured and excluded from total pellet area after equally setting the thresholding using ImageJ software. (F) Quantitative summary of adipogenic differentiation showing the number of oil-red positive cells counted from 64 images taken under 10× magnification using Image Xpress Micro 4. (G) Quantitative summary of osteogenic differentiation showing alizarin red-positive area semi manually measured from at least 10 images using ImageJ software. Data are presented as mean ± SEM from four independent samples. ns, not significant.

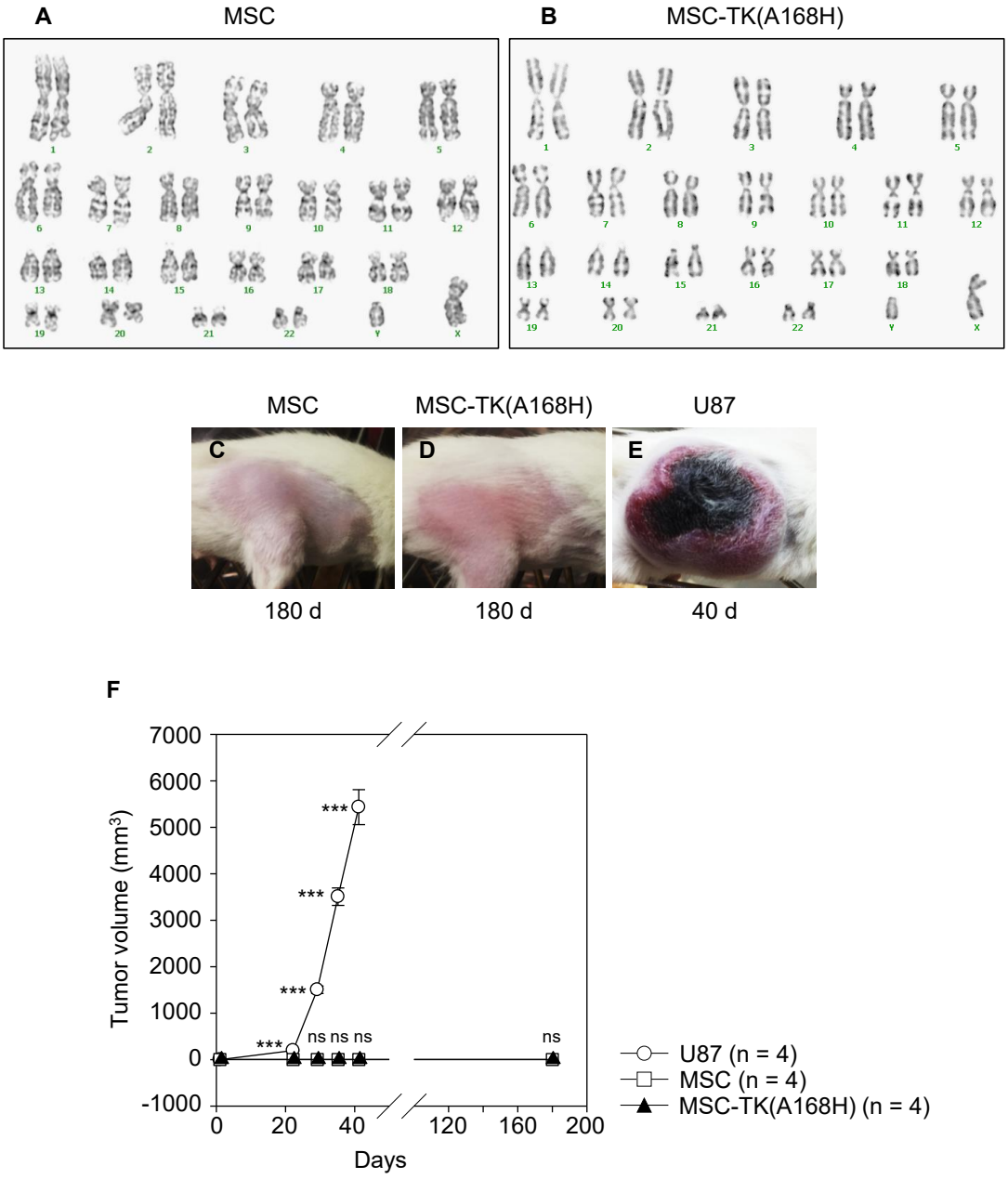

Fig. 4. Genetic stability and safety of MSC-TK(A168H). (A and B) G-banding assay indicating a normal (46, XY) karyotype in MSC and MSC-TK(A168H) at P7. (C and D) MSCs and MSC-TK(A168H) cells did not form tumors 180 days after 10^6 cells were subcutaneously injected in NSG mice. (E) U87 cells, a positive control, formed tumors within 40 days. (F) U87-tumor volume was weekly measured at day 0, 21, 28, 35, and 40 from four animals according to following formula: volume = $\pi/6 \times L \times W \times H$. Data are presented mean ± SEM from 4 animals per group (***$P < 0.001$ compared to MSC group; Student's *t*-test). ns, not significant.

a prodrug for GCV, was first determined in nude mice. After the tumor volume reached approximately 100-300 mm^3, vGCV was administered orally at doses of 50, 200, 400, or 800 mg/kg once per day for 14 days. Within 4 days after drug administration, the tumor volume was reduced by more than 90% (dotted line) with 200, 400, and 800 mg/kg doses of vGCV, whereas it took 12 days to lower the tumor volume to 90% with the 50 mg/kg dose (Figs. 6A and 6B). The data indicate that vGCV cleared TK-bearing tumors in a dose-dependent manner. It should be noted that doses higher than 200 mg/kg induced severe body weight loss (Fig. 6C). These results suggest that 200 mg/kg vGCV may be an effective dose to clear tumors rapidly without toxicity (weight loss).

To compare the direct effect of TK and TK(A168H) with GCV while eliminating potential contributions of the secondary effects of the host immune system, we performed similar

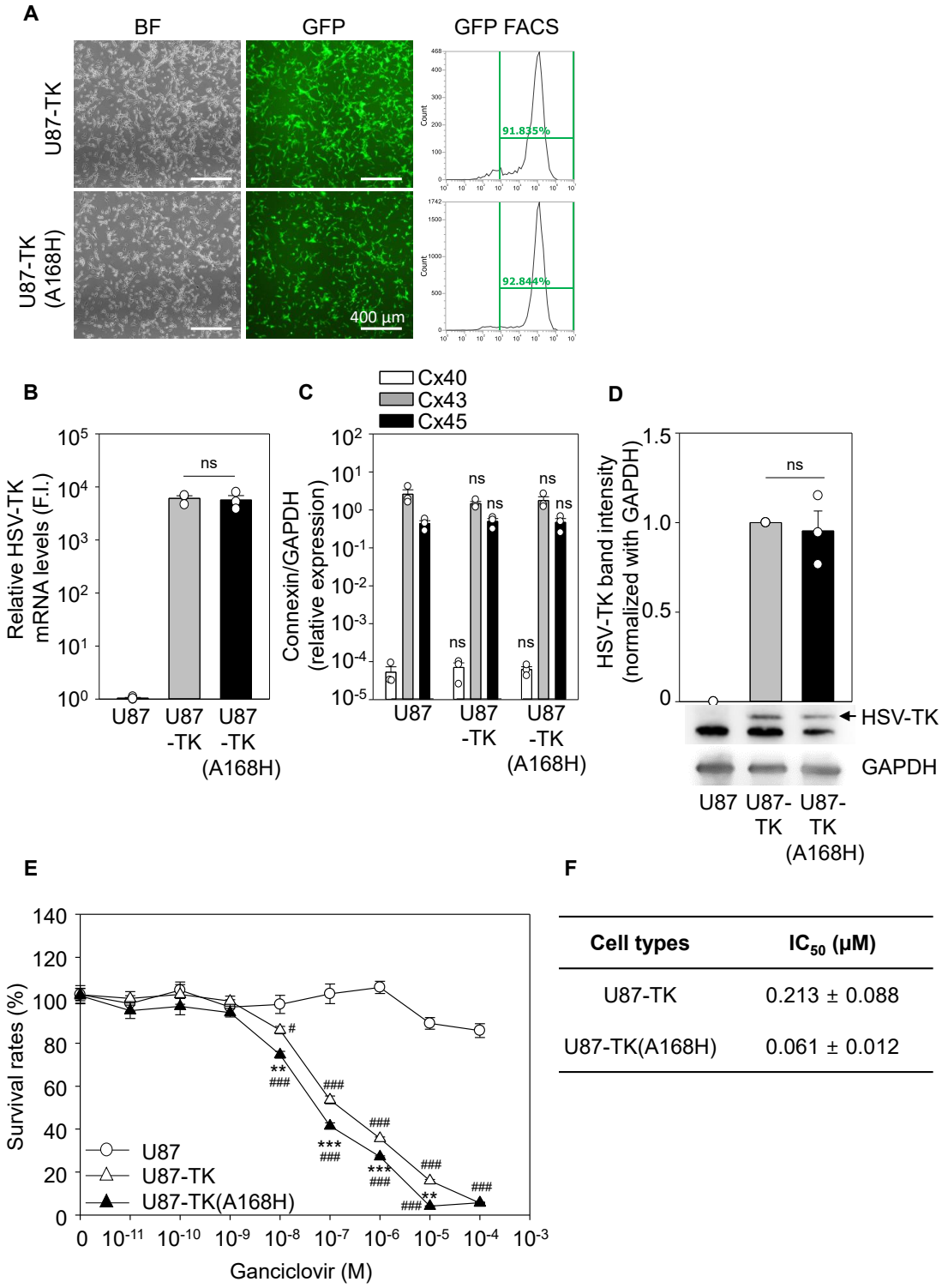

Fig. 5. Cytotoxic effects of GCV on U87-TK(A168H). (A) Phase contrast and fluorescence images of U87 cells transduced with lentivirus encoding CopGFP and either WT HSV-TK or HSV-TK(A168H). FACS analysis showing the copGFP-positive cells and transduction efficiency. (B) RT-qPCR analysis indicating similar levels TK gene expression (fold induction; F.I.) in U87-TK and U87-TK(A168H) in comparison to naïve U87 cells. (C) RT-qPCR analysis showing higher Cx43 and Cx45, but minimal levels of Cx40 in U87 based cell lines. (D) Western blot analysis showing relative levels of TK protein expression in transduced cells. GAPDH was used as a loading control. (E) MTT assays indicating the cytotoxic effect of GCV on U87-TK and U87-TK(A168H) cells. (F) IC_{50} values for GCV in U87-TK and U87-TK(A168H) cells. Data are presented as mean ± SEM from at least three independent samples ($^{\#}P < 0.05$, $^{\#\#\#}P < 0.001$ compared to U87; $^{**}P < 0.01$, $^{***}P < 0.001$ compared to U87-TK group; one-way ANOVA test). ns, not significant.

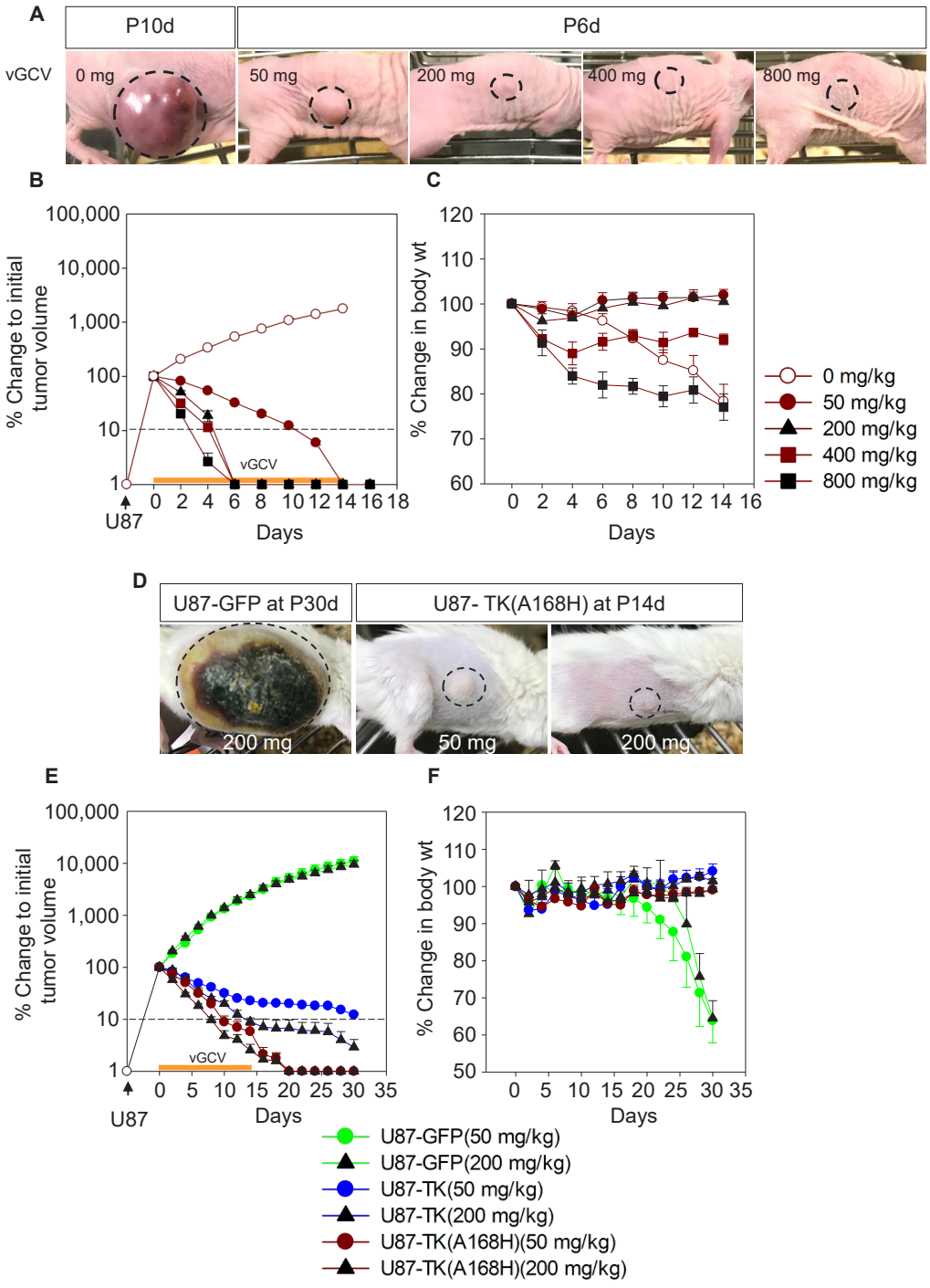

Fig. 6. Modeling SAE with U87-derived cells and suppressing the uncontrolled cell growth *in vivo*. (A) Representative images of U87-TK(A168H) tumor 6 days after daily administration of 50, 200, 400, and 800 mg/kg vGCV. Tumor sites are demarcated with dotted circles. The image of saline (0 mg) group was 10 days after drug administration. (B) Decrease in tumor volume indicating the clearance of tumors at various rates by administration of doses of vGCV (orange line). (C) Body weight is presented after subtracting tumor mass, indicating toxicity of vGCV at doses higher than 200 mg/kg. Data are presented mean ± SEM from four animals per group. (D) Representative images of U87-TK(A168H) 14 days after vGCV administration in NSG mice. The growth of U87-GFP without TK was not suppressed at 30 days after 200 mg/kg vGCV treatment. Tumor sites are demarcated with dotted circles. (E) Cytotoxic effect of TK and TK(A168H) *in vivo* in combination with daily administration of 50 and 200 mg/kg vGCV for 14 days (orange line). Note that tumors with U87-GFP without TK continuously grew in the presence of vGCV. (F) Body weight is presented after subtracting tumor mass, indicating the 200 mg/kg are tolerable. Weight loss was severe in the U87-GFP without TK due to heavy tumor burden. Data are presented mean ± SEM from 3-6 animals per group. Figures with statistical significance for Figs. 6B, 6C, 6E, and 6F is in Supplementary Figs. S2A-S2D, respectively.

experiments in NSG mice in which B-, T-, and natural killer (NK)-cell development were severely impaired. Administration of 50-200 mg/kg vGCV lowered the tumor volume more effectively in the U87-TK(A168H) group than in the U87-TK group. In the U87-TK(A168H) group, it took 10 and 8 days to clear 90% of the initial tumor volume with 50 and 200 mg/kg, respectively (Fig. 6E). With the same doses of vGCV, it took 35 and 15 days to clear the tumor volume by more than 90% in the U87-TK group. As in nude mice, vGCV itself did not cause any weight loss at these doses (Fig. 6F). One animal each in the U87-TK and U87-TK(A168H) groups at 50 mg/kg showed tumor recurrence 62 and 70 days, respectively, after the last GCV administration, indicating that 50 mg/kg was not sufficient to completely eradicate tumor cells. Importantly tumor recurrence was never observed at 200 mg/kg up to 120 days after the last day of administration. These findings indicate that 200 mg/kg vGCV is sufficient to completely clear tumors without any obvious side effects. Hence, using the TK(A168H) mutant as a safety gene provides a way to prevent and cure possible tumorigenesis from transplanted cells in the *ex vivo* therapy. In contrast, vGCV did not have a tumor-suppressive effect in the absence of TK, such as in the U87-GFP group, where the tumor volume increased rapidly with severe weight loss in the animals (Figs. 6D and 6E), supporting the preclinical relevance of our approach. The mice were euthanized at day 30 after treatment because they became immobilized as a result of high tumor burden.

DISCUSSION

MSCs have been studied as drugs for cell-based therapies in a variety of disorders, such as tissue damage and degenerative diseases, but their efficacy is controversial. Disease-specific therapeutic genes have been introduced into MSCs via retrovirus and lentivirus to enhance the therapeutic potency of MSCs. A positive aspect of these chromosomally inserting viral vectors is that they allow for sustained expression of therapeutic genes to obtain uniformly competent cells after large-scale production. However, chromosomal integration can alter stem cell characteristics and cause unexpected SAEs. This study demonstrates the potential use of the HSV-TK(A168H) gene as an efficient safety switch to manage the potential risk of SAEs in lentivirus-based *ex vivo* therapy.

Undifferentiated MSCs express human leukocyte antigen (HLA) class I, but not class II, such as HLA-DR (Le Blanc et al., 2003). The hypoimmunogenic nature of MSCs makes allogeneic transplantation feasible and makes them attractive as off-the-shelf therapeutics. In this study, we show that lentiviral transduction by itself does not alter the hypoimmunogenic properties of MSCs, and the resulting *ex vivo* therapy can result in transplantable allogeneic cells.

Transduction of viral vectors may alter stem cell properties of MSCs. As mentioned earlier, using adenovirus at high MOI affects the growth and adipogenic differentiation of MSCs (Marasini et al., 2017). In contrast, transduction of lentiviral vectors did not interfere with the proliferation of MSC-TK(A168H) cells, and their growth eventually stopped after long-term culture, indicating that lentiviral transduction did not cause any malignant transformation (Fig. 2A). Consistent with these results, karyotyping analysis did not reveal any chromosomal instability (Fig. 4). Moreover, MSCs and MSC-TK(A168H) cells did not form solid tumors in NSG mice for 180 days after subcutaneous injection (Fig. 4). Taken together, these results indicate that lentivirus-based MSCs are safe in preclinical conditions. Previously, although retroviral transduction by itself did not alter the stem cell properties of MSCs (Park et al., 2013), retrovirus-mediated overexpression of a neurogenic transcription factor, neurogenin 1 (Ngn1), converts MSC fate from mesodermal to neuronal lineage (Kim et al., 2008). Therefore, it is possible that the mesodermal properties of MSCs can be affected by therapeutic genes loaded into the lentiviral vector. For example, lentiviral vectors encoding TRAF4 (TNF receptor-associated factor 4), p130 (a member of the retinoblastoma gene product, pRb), E2F4 (a transcriptional repressor), and microRNA-410 alter the differentiation potential of MSCs (Cen et al., 2020; Zhang et al., 2017; 2018). In contrast with these findings, we found that TK(A168H) overexpression did not alter the adipogenic, osteogenic, and chondrogenic differentiation potential of MSCs. Hence, the TK(A168H) gene can be utilized together with other therapeutic genes while preserving the differentiation ability of MSCs.

Although MSCs are known to be clinically safe, MSC-based *ex vivo* therapies can carry a potential risk of side effects, such as uncontrolled growth of treated cells. For this, we explored the use of the HSV-TK gene as a safety gene. HSV-TK recognizes both thymidine and GCV, a guanine nucleoside analog (Balzarini et al., 2006). The preference for substrate phosphorylation towards GCV or ACV, rather than thymidine, is essential for efficiently inducing apoptosis with low drug doses. For this purpose, several active site mutations such as TK30, TK75, and SR39 have been explored. Although these mutations lower catalytic activity, they all render the cells more sensitive to GCV than WT-TK by reducing K_m values for GCV or increasing K_m for thymidine, an internal competitor for GCV (Black et al., 1996; 2001). In comparison, the A168H substitution increased both catalytic activity and the GCV selectivity by 4-fold against thymidine compared to the WT, making it more suitable as a safety switch compared to WT-TK (Balzarini et al., 2006). In line with this notion, TK(A168H) confers higher responsiveness to GCV in both MSCs and U87 as assessed by *in vitro* MTT assays (Figs. 1 and 5). Because the expression levels of WT-TK and TK(A168H) were similar in the two cell lines, the lower IC_{50} was attributed to the higher GCV substrate affinity of TK with the A168H substitution than WT-TK. In contrast, fully codon-optimized HSV-TK(A168H) had a higher expression level than codon-optimized TK and splice-corrected TK in K562 (immune) cells (Preuss et al., 2010). We used TK with an A168H substitution without codon optimization and splice correction transduced into stem cells using lentivirus. The variations in expression between our system and other reports in the literature might be caused either by modification of TK, different viral vectors used, or context-dependent cell-type dependent variations. Two TK specific bands were detected in MSC-TK and MSC-TK(A168H) cells whereas only one band in U87-TK and U87-TK(A168H) cells (compare Figs. 1E and 5D). The variations in TK protein expression might be caused by cell type-specific

initiation of translation mainly from the second internal ATG codon of the TK gene (al-Shawi et al., 1991; Marsden et al., 1983).

Ex vivo gene therapy was originally initiated with hematopoietic stem cells (HSCs) to cure monogenic genetic diseases, including adenosine deaminase severe combined immunodeficiency (ADA-SCID), X-linked-SCID, and X-linked adrenoleukodystrophy (ALD) (Cartier et al., 2009; Cicalese et al., 2018; Hacein-Bey-Abina et al., 2002; Naldini, 2011; Tani, 2016). Recently, chimeric antigen receptor (CAR)-T cells have emerged as a powerful treatment for acute lymphocytic leukemia (Kalos et al., 2011). SAEs have been reported as biased differentiation of HSCs, resulting in the development of leukemia for HSC-based therapy (Hacein-Bey-Abina et al., 2014) and cytokine release syndrome for CAR-T cell therapy (Fitzgerald et al., 2017; Locke et al., 2019; Neelapu et al., 2017; Schuster et al., 2019; Wang et al., 2020). Based on its superior performance, TK(A168H) represents a promising alternative to mitigate SAEs. TK(A168H) may be beneficial for reducing or clearing transplanted cells.

Although vGCV $\geq$ 200 mg/kg can completely ablate tumors, it takes 6 and 20 days in nude and NSG mice, respectively (compare Figs. 6B and 6E). The delayed response in NSG mice could be attributed to the fact that B-, T-, and NK-cell development is impaired in NSG mice, whereas only T-cell development is impaired in nude mice (Belizário, 2009). The data also suggest that immune cell contribution may play a secondary role in suppressing tumor growth. Our finding is in line with a previous report that HSV-TK/GCV induces antitumor NK cell activity in an orthotopic mouse model of prostate cancer (Hall et al., 1998). Taken together, rapid tumor ablation in nude mice compared to NSG mice can be enhanced by a combination of activated NK cells and HSV-TK/GCV-mediated apoptosis. NSG mice, rather than nude mouse-based xenograft models, is the preferred model to find the primary antitumor effects of new therapeutic agents without the involvement of secondary effects by NK cells.

Transducing cultured cells results in MSC-TK or MSC-TK(A168H) cells representing 56%-58% of the total cells, and the remaining cells do not express TK. GCV added to the culture exerted cytotoxicity to both TK-expressing and non-TK-expressing cells in the MTT assay (Figs. 1F and 1G). Because phosphorylated GCV molecules are polar and cannot penetrate the cell membrane, they exert effects by entering cells through gap junctions (Mesnil and Yamasaki, 2000; van Dillen et al., 2002). Indeed, MSCs express major components of gap junctions, such as Cx43, Cx40, and Cx45, and communicate with neighboring cells through gap junctions (Dilger et al., 2020; Valiunas et al., 2004). In this study, MSCs, MSC-TK, and MSC-TK(A168H) cells expressed high levels of Cx43 and Cx45 but minimally expressed Cx40 (Fig. 1D), which causes untransduced, TK-negative, copGFP-negative cells to be affected by GCV.

In MSC-TK cells, GFP was used as a surrogate gene instead of therapeutic genes of interest. Although MSC-TK cells are not oncogenic in pre-clinical study, introducing other therapeutic genes in MSC-based *ex-vivo* therapy may provoke SAE in real world. As regulatory bodies (U.S. Food and Drug Administration [FDA], European Medicines Agency [EMA], Ministry of Food and Drug Safety [MFDS], etc.) are likely to require a strategy to end or mitigate SAEs in the future approval phase, it is necessary to equip safety switches such as TK gene from the early stages of development.

Similar mutant TK.007, a codon optimized TK(A168H) has been previously tested as a safety switch to abolish SAE in blood cell-based *ex-vivo* therapy (Preuss et al., 2010). In a GvHD model, freely mobile blood cells containing TK.007 can be removed by intraperitoneal injection of GCV. Like in hematological SAEs, like GvHD, we showed that TK(A168H) could function as a safety switch to mitigate SAEs of transformation to solid cancers in MSC-based *ex-vivo* therapy. TK activity as a safety switch is usually not required in normal situations, which differs from TK gene cancer therapy in which TK activity is required to kill cancer cells throughout the therapeutic period (Preuss et al., 2010).

In summary, MSCs are clinically safe and are used worldwide. Attempts have been made to enhance therapeutic efficacy by introducing functional genes into MSCs. Including TK(A168H) in the viral vectors along with functional genes to enhance the therapeutic potential in the early development of viral vectors may be a promising strategy while achieving the high clinical safety standard of MSC-based *ex vivo* therapy.

Note: Supplementary information is available on the Molecules and Cells website (www.molcells.org).

ACKNOWLEDGMENTS

This research was supported by grants from the Korea Health Technology R&D Project through the Korea Health Industry Development Institute (KHIDI), funded by the Ministry of Health & Welfare (HI20C0457 to H.S.K.), the Ministry of Food and Drug Safety in 2021 (18172MFDS182-5 to H.S.K.) and the Technology development Program (S3030270 to D.Y.C.) funded by the Ministry of SMEs and Startups (MSS, Korea).

AUTHOR CONTRIBUTIONS

N.B. and T.Y.L. wrote the manuscript. N.B., T.Y.L., D.Y.C., and J.H.J. performed experiments. N.B., T.Y.L., D.Y.C., J.H.J., M.G.K., R.A., and S.S.K. analyzed the data. I.H.O. and H.S.K. provided funding and supervised the research. All authors read and approved the manuscript.

CONFLICT OF INTEREST

T.Y.L., D.Y.C., and H.S.K. are employees of and stock and/or option holders in Cell&Brain Co., Ltd. The other authors have no potential conflicts of interest to disclose.

ORCID

Narayan Bashyal https://orcid.org/0000-0001-8531-8058
Tae-Young Lee https://orcid.org/0000-0002-9697-2765
Da-Young Chang https://orcid.org/0000-0002-9419-2618
Jin-Hwa Jung https://orcid.org/0000-0003-0940-8566
Min Gyeong Kim https://orcid.org/0000-0002-1446-6720
Rakshya Acharya https://orcid.org/0000-0001-7215-498X
Sung-Soo Kim https://orcid.org/0000-0003-3591-5932
Il-Hoan Oh https://orcid.org/0000-0002-0034-3340
Haeyoung Suh-Kim https://orcid.org/0000-0001-8175-1209

REFERENCES

al-Shawi, R., Burke, J., Wallace, H., Jones, C., Harrison, S., Buxton, D., Maley, S., Chandley, A., and Bishop, J.O. (1991). The herpes simplex virus type 1 thymidine kinase is expressed in the testes of transgenic mice under the control of a cryptic promoter. Mol. Cell. Biol. *11*, 4207-4216.

Aurich, H., Sgodda, M., Kaltwasser, P., Vetter, M., Weise, A., Liehr, T., Brulport, M., Hengstler, J.G., Dollinger, M.M., Fleig, W.E., et al. (2009). Hepatocyte differentiation of mesenchymal stem cells from human adipose tissue in vitro promotes hepatic integration in vivo. Gut *58*, 570-581.

Balzarini, J., Liekens, S., Solaroli, N., El Omari, K., Stammers, D.K., and Karlsson, A. (2006). Engineering of a single conserved amino acid residue of herpes simplex virus type 1 thymidine kinase allows a predominant shift from pyrimidine to purine nucleoside phosphorylation. J. Biol. Chem. *281*, 19273-19279.

Belizário, J.E. (2009). Immunodeficient mouse models: an overview. Open Immunol. J. *2*, 79-85.

Beltinger, C., Fulda, S., Kammertoens, T., Meyer, E., Uckert, W., and Debatin, K.M. (1999). Herpes simplex virus thymidine kinase/ganciclovir-induced apoptosis involves ligand-independent death receptor aggregation and activation of caspases. Proc. Natl. Acad. Sci. U. S. A. *96*, 8699-8704.

Black, M.E., Kokoris, M.S., and Sabo, P. (2001). Herpes simplex virus-1 thymidine kinase mutants created by semi-random sequence mutagenesis improve prodrug-mediated tumor cell killing. Cancer Res. *61*, 3022-3026.

Black, M.E., Newcomb, T.G., Wilson, H.M., and Loeb, L.A. (1996). Creation of drug-specific herpes simplex virus type 1 thymidine kinase mutants for gene therapy. Proc. Natl. Acad. Sci. U. S. A. *93*, 3525-3529.

Cartier, N., Hacein-Bey-Abina, S., Bartholomae, C.C., Veres, G., Schmidt, M., Kutschera, I., Vidaud, M., Abel, U., Dal-Cortivo, L., Caccavelli, L., et al. (2009). Hematopoietic stem cell gene therapy with a lentiviral vector in X-linked adrenoleukodystrophy. Science *326*, 818-823.

Cen, S., Li, J., Cai, Z., Pan, Y., Sun, Z., Li, Z., Ye, G., Zheng, G., Li, M., Liu, W., et al. (2020). TRAF4 acts as a fate checkpoint to regulate the adipogenic differentiation of MSCs by activating PKM2. EBioMedicine *54*, 102722.

Chang, D.Y., Jung, J.H., Kim, A.A., Marasini, S., Lee, Y.J., Paek, S.H., Kim, S.S., and Suh-Kim, H. (2020). Combined effects of mesenchymal stem cells carrying cytosine deaminase gene with 5-fluorocytosine and temozolomide in orthotopic glioma model. Am. J. Cancer Res. *10*, 1429-1441.

Chang, D.Y., Yoo, S.W., Hong, Y., Kim, S., Kim, S.J., Yoon, S.H., Cho, K.G., Paek, S.H., Lee, Y.D., Kim, S.S., et al. (2010). The growth of brain tumors can be suppressed by multiple transplantation of mesenchymal stem cells expressing cytosine deaminase. Int. J. Cancer *127*, 1975-1983.

Cicalese, M.P., Ferrua, F., Castagnaro, L., Rolfe, K., De Boever, E., Reinhardt, R.R., Appleby, J., Roncarolo, M.G., and Aiuti, A. (2018). Gene therapy for adenosine deaminase deficiency: a comprehensive evaluation of short- and medium-term safety. Mol. Ther. *26*, 917-931.

De Ravin, S.S., Wu, X., Moir, S., Anaya-O'Brien, S., Kwatemaa, N., Littel, P., Theobald, N., Choi, U., Su, L., Marquesen, M., et al. (2016). Lentiviral hematopoietic stem cell gene therapy for X-linked severe combined immunodeficiency. Sci. Transl. Med. *8*, 335ra357.

Dilger, N., Neehus, A.L., Grieger, K., Hoffmann, A., Menssen, M., and Ngezahayo, A. (2020). Gap junction dependent cell communication is modulated during transdifferentiation of mesenchymal stem/stromal cells towards neuron-like cells. Front. Cell Dev. Biol. *8*, 869.

Dos Santos, J.F., Borçari, N.R., da Silva Araújo, M., and Nunes, V.A. (2019). Mesenchymal stem cells differentiate into keratinocytes and express epidermal kallikreins: towards an in vitro model of human epidermis. J. Cell. Biochem. *120*, 13141-13155.

Field, A.K., Davies, M.E., DeWitt, C., Perry, H.C., Liou, R., Germershausen, J., Karkas, J.D., Ashton, W.T., Johnston, D.B., and Tolman, R.L. (1983). 9-([2-hydroxy-1-(hydroxymethyl)ethoxy]methyl)guanine: a selective inhibitor of herpes group virus replication. Proc. Natl. Acad. Sci. U. S. A. *80*, 4139-4143.

Fitzgerald, J.C., Weiss, S.L., Maude, S.L., Barrett, D.M., Lacey, S.F., Melenhorst, J.J., Shaw, P., Berg, R.A., June, C.H., Porter, D.L., et al. (2017). Cytokine release syndrome after chimeric antigen receptor T cell therapy for acute lymphoblastic leukemia. Crit. Care Med. *45*, e124-e131.

Greco, R., Oliveira, G., Stanghellini, M.T., Vago, L., Bondanza, A., Peccatori, J., Cieri, N., Marktel, S., Mastaglio, S., Bordignon, C., et al. (2015). Improving the safety of cell therapy with the TK-suicide gene. Front. Pharmacol. *6*, 95.

Hacein-Bey-Abina, S., Le Deist, F., Carlier, F., Bouneaud, C., Hue, C., De Villartay, J.P., Thrasher, A.J., Wulffraat, N., Sorensen, R., Dupuis-Girod, S., et al. (2002). Sustained correction of X-linked severe combined immunodeficiency by ex vivo gene therapy. N. Engl. J. Med. *346*, 1185-1193.

Hacein-Bey-Abina, S., Pai, S.Y., Gaspar, H.B., Armant, M., Berry, C.C., Blanche, S., Bleesing, J., Blondeau, J., de Boer, H., Buckland, K.F., et al. (2014). A modified γ-retrovirus vector for X-linked severe combined immunodeficiency. N. Engl. J. Med. *371*, 1407-1417.

Hall, S.J., Sanford, M.A., Atkinson, G., and Chen, S.H. (1998). Induction of potent antitumor natural killer cell activity by herpes simplex virus-thymidine kinase and ganciclovir therapy in an orthotopic mouse model of prostate cancer. Cancer Res. *58*, 3221-3225.

Hetzel, M., Suzuki, T., Hashtchin, A.R., Arumugam, P., Carey, B., Schwabbauer, M., Kuhn, A., Meyer, J., Schambach, A., Van Der Loo, J., et al. (2017). Function and safety of lentivirus-mediated gene transfer for CSF2RA-deficiency. Hum. Gene Ther. Methods *28*, 318-329.

Huang, P., Wang, L., Li, Q., Xu, J., Xu, J., Xiong, Y., Chen, G., Qian, H., Jin, C., Yu, Y., et al. (2019). Combinatorial treatment of acute myocardial infarction using stem cells and their derived exosomes resulted in improved heart performance. Stem Cell Res. Ther. *10*, 300.

Kalos, M., Levine, B.L., Porter, D.L., Katz, S., Grupp, S.A., Bagg, A., and June, C.H. (2011). T cells with chimeric antigen receptors have potent antitumor effects and can establish memory in patients with advanced leukemia. Sci. Transl. Med. *3*, 95ra73.

Kan, I., Ben-Zur, T., Barhum, Y., Levy, Y.S., Burstein, A., Charlow, T., Bulvik, S., Melamed, E., and Offen, D. (2007). Dopaminergic differentiation of human mesenchymal stem cells--utilization of bioassay for tyrosine hydroxylase expression. Neurosci. Lett. *419*, 28-33.

Kim, S.S., Choi, J.M., Kim, J.W., Ham, D.S., Ghil, S.H., Kim, M.K., Kim-Kwon, Y., Hong, S.Y., Ahn, S.C., Kim, S.U., et al. (2005). cAMP induces neuronal differentiation of mesenchymal stem cells via activation of extracellular signal-regulated kinase/MAPK. Neuroreport *16*, 1357-1361.

Kim, S.S., Kim, B.J., and Suh-Kim, H. (2003). The efficient gene delivery into human mesenchymal stem cells using retroviral vectors. Korean J. Anat. *36*, 381-387.

Kim, S.S., Yoo, S.W., Park, T.S., Ahn, S.C., Jeong, H.S., Kim, J.W., Chang, D.Y., Cho, K.G., Kim, S.U., Huh, Y., et al. (2008). Neural induction with neurogenin1 increases the therapeutic effects of mesenchymal stem cells in the ischemic brain. Stem Cells *26*, 2217-2228.

Le Blanc, K., Rasmusson, I., Sundberg, B., Götherström, C., Hassan, M., Uzunel, M., and Ringdén, O. (2004). Treatment of severe acute graft-versus-host disease with third party haploidentical mesenchymal stem cells. Lancet *363*, 1439-1441.

Le Blanc, K., Tammik, C., Rosendahl, K., Zetterberg, E., and Ringdén, O. (2003). HLA expression and immunologic propertiesof differentiated and undifferentiated mesenchymal stem cells. Exp. Hematol. *31*, 890-896.

Lee, S.H., Jin, K.S., Bang, O.Y., Kim, B.J., Park, S.J., Lee, N.H., Yoo, K.H., Koo, H.H., and Sung, K.W. (2015). Differential migration of mesenchymal stem cells to ischemic regions after middle cerebral artery occlusion in rats.

PLoS One *10*, e0134920.

Lee, T.Y., Cho, I.S., Bashyal, N., Naya, F.J., Tsai, M.J., Yoon, J.S., Choi, J.M., Park, C.H., Kim, S.S., and Suh-Kim, H. (2020). ERK regulates NeuroD1-mediated neurite outgrowth via proteasomal degradation. Exp. Neurobiol. *29*, 189-206.

Lin, P., Lin, Y., Lennon, D.P., Correa, D., Schluchter, M., and Caplan, A.I. (2012). Efficient lentiviral transduction of human mesenchymal stem cells that preserves proliferation and differentiation capabilities. Stem Cells Transl. Med. *1*, 886-897.

Locke, F.L., Ghobadi, A., Jacobson, C.A., Miklos, D.B., Lekakis, L.J., Oluwole, O.O., Lin, Y., Braunschweig, I., Hill, B.T., Timmerman, J.M., et al. (2019). Long-term safety and activity of axicabtagene ciloleucel in refractory large B-cell lymphoma (ZUMA-1): a single-arm, multicentre, phase 1-2 trial. Lancet Oncol. *20*, 31-42.

Ma, T., Gong, K., Ao, Q., Yan, Y., Song, B., Huang, H., Zhang, X., and Gong, Y. (2013). Intracerebral transplantation of adipose-derived mesenchymal stem cells alternatively activates microglia and ameliorates neuropathological deficits in Alzheimer's disease mice. Cell Transplant. *22* Suppl 1, S113-S126.

Marasini, S., Chang, D.Y., Jung, J.H., Lee, S.J., Cha, H.L., Suh-Kim, H., and Kim, S.S. (2017). Effects of adenoviral gene transduction on the stemness of human bone marrow mesenchymal stem cells. Mol. Cells *40*, 598-605.

Marsden, H.S., Haarr, L., and Preston, C.M. (1983). Processing of herpes simplex virus proteins and evidence that translation of thymidine kinase mRNA is initiated at three separate AUG codons. J. Virol. *46*, 434-445.

Mazzini, L., Fagioli, F., Boccaletti, R., Mareschi, K., Oliveri, G., Olivieri, C., Pastore, I., Marasso, R., and Madon, E. (2003). Stem cell therapy in amyotrophic lateral sclerosis: a methodological approach in humans. Amyotroph. Lateral Scler. Other Motor Neuron Disord. *4*, 158-161.

McGarrity, G.J., Hoyah, G., Winemiller, A., Andre, K., Stein, D., Blick, G., Greenberg, R.N., Kinder, C., Zolopa, A., Binder-Scholl, G., et al. (2013). Patient monitoring and follow-up in lentiviral clinical trials. J. Gene Med. *15*, 78-82.

Mesnil, M. and Yamasaki, H. (2000). Bystander effect in herpes simplex virus-thymidine kinase/ganciclovir cancer gene therapy: role of gap-junctional intercellular communication. Cancer Res. *60*, 3989-3999.

Naldini, L. (2011). Ex vivo gene transfer and correction for cell-based therapies. Nat. Rev. Genet. *12*, 301-315.

Neelapu, S.S., Locke, F.L., Bartlett, N.L., Lekakis, L.J., Miklos, D.B., Jacobson, C.A., Braunschweig, I., Oluwole, O.O., Siddiqi, T., Lin, Y., et al. (2017). Axicabtagene ciloleucel CAR T-cell therapy in refractory large B-cell lymphoma. N. Engl. J. Med. *377*, 2531-2544.

Park, J.S., Chang, D.Y., Kim, J.H., Jung, J.H., Park, J., Kim, S.H., Lee, Y.D., Kim, S.S., and Suh-Kim, H. (2013). Retrovirus-mediated transduction of a cytosine deaminase gene preserves the stemness of mesenchymal stem cells. Exp. Mol. Med. *45*, e10.

Park, J.S., Suryaprakash, S., Lao, Y.H., and Leong, K.W. (2015). Engineering mesenchymal stem cells for regenerative medicine and drug delivery. Methods *84*, 3-16.

Pittenger, M.F., Mackay, A.M., Beck, S.C., Jaiswal, R.K., Douglas, R., Mosca, J.D., Moorman, M.A., Simonetti, D.W., Craig, S., and Marshak, D.R. (1999). Multilineage potential of adult human mesenchymal stem cells. Science *284*, 143-147.

Poudineh, M., Wang, Z., Labib, M., Ahmadi, M., Zhang, L., Das, J., Ahmed, S., Angers, S., and Kelley, S.O. (2018). Three-dimensional nanostructured architectures enable efficient neural differentiation of mesenchymal stem cells via mechanotransduction. Nano Lett. *18*, 7188-7193.

Preuss, E., Treschow, A., Newrzela, S., Brücher, D., Weber, K., Felldin, U., Alici, E., Gahrton, G., von Laer, D., Dilber, M.S., et al. (2010). TK.007: a novel, codon-optimized HSVtk(A168H) mutant for suicide gene therapy. Hum. Gene Ther. *21*, 929-941.

Ramos, C.A., Asgari, Z., Liu, E., Yvon, E., Heslop, H.E., Rooney, C.M., Brenner, M.K., and Dotti, G. (2010). An inducible caspase 9 suicide gene to improve the safety of mesenchymal stromal cell therapies. Stem Cells *28*, 1107-1115.

Reardon, J.E. (1989). Herpes simplex virus type 1 and human DNA polymerase interactions with 2′-deoxyguanosine 5′-triphosphate analogues. Kinetics of incorporation into DNA and induction of inhibition. J. Biol. Chem. *264*, 19039-19044.

Rothenburger, T., Thomas, D., Schreiber, Y., Wratil, P.R., Pflantz, T., Knecht, K., Digianantonio, K., Temple, J., Schneider, C., Baldauf, H.M., et al. (2021). Differences between intrinsic and acquired nucleoside analogue resistance in acute myeloid leukaemia cells. J. Exp. Clin. Cancer Res. *40*, 317.

Schuster, S.J., Bishop, M.R., Tam, C.S., Waller, E.K., Borchmann, P., McGuirk, J.P., Jäger, U., Jaglowski, S., Andreadis, C., Westin, J.R., et al. (2019). Tisagenlecleucel in adult relapsed or refractory diffuse large B-cell lymphoma. N. Engl. J. Med. *380*, 45-56.

Sgodda, M., Aurich, H., Kleist, S., Aurich, I., König, S., Dollinger, M.M., Fleig, W.E., and Christ, B. (2007). Hepatocyte differentiation of mesenchymal stem cells from rat peritoneal adipose tissue in vitro and in vivo. Exp. Cell Res. *313*, 2875-2886.

Shin, J.W., Ryu, S., Ham, J., Jung, K., Lee, S., Chung, D.H., Kang, H.R., and Kim, H.Y. (2021). Mesenchymal stem cells suppress severe asthma by directly regulating Th2 cells and type 2 innate lymphoid cells. Mol. Cells *44*, 580-590.

Suzuki, M., McHugh, J., Tork, C., Shelley, B., Hayes, A., Bellantuono, I., Aebischer, P., and Svendsen, C.N. (2008). Direct muscle delivery of GDNF with human mesenchymal stem cells improves motor neuron survival and function in a rat model of familial ALS. Mol. Ther. *16*, 2002-2010.

Szaraz, P., Gratch, Y.S., Iqbal, F., and Librach, C.L. (2017). In vitro differentiation of human mesenchymal stem cells into functional cardiomyocyte-like cells. J. Vis. Exp. *(126)*, 55757.

Tani, K. (2016). Current status of ex vivo gene therapy for hematological disorders: a review of clinical trials in Japan around the world. Int. J. Hematol. *104*, 42-72.

Tomayko, M.M. and Reynolds, C.P. (1989). Determination of subcutaneous tumor size in athymic (nude) mice. Cancer Chemother. Pharmacol. *24*, 148-154.

Unsal, I.O., Ginis, Z., Pinarli, F.A., Albayrak, A., Cakal, E., Sahin, M., and Delibasi, T. (2015). Comparison of therapeutic characteristics of islet cell transplantation simultaneous with pancreatic mesenchymal stem cell transplantation in rats with Type 1 diabetes mellitus. Stem Cell Rev. Rep. *11*, 526-532.

Valiunas, V., Doronin, S., Valiuniene, L., Potapova, I., Zuckerman, J., Walcott, B., Robinson, R.B., Rosen, M.R., Brink, P.R., and Cohen, I.S. (2004). Human mesenchymal stem cells make cardiac connexins and form functional gap junctions. J. Physiol. *555*, 617-626.

van Dillen, I.J., Mulder, N.H., Vaalburg, W., de Vries, E.F., and Hospers, G.A. (2002). Influence of the bystander effect on HSV-tk/GCV gene therapy. A review. Curr. Gene Ther. *2*, 307-322.

Wang, F., Yasuhara, T., Shingo, T., Kameda, M., Tajiri, N., Yuan, W.J., Kondo, A., Kadota, T., Baba, T., Tayra, J.T., et al. (2010). Intravenous administration of mesenchymal stem cells exerts therapeutic effects on parkinsonian model of rats: focusing on neuroprotective effects of stromal cell-derived factor-1alpha. BMC Neurosci. *11*, 52.

Wang, M., Munoz, J., Goy, A., Locke, F.L., Jacobson, C.A., Hill, B.T., Timmerman, J.M., Holmes, H., Jaglowski, S., Flinn, I.W., et al. (2020). KTE-X19 CAR T-cell therapy in relapsed or refractory mantle-cell lymphoma. N. Engl. J. Med. *382*, 1331-1342.

Xin, H., Li, Y., Cui, Y., Yang, J.J., Zhang, Z.G., and Chopp, M. (2013). Systemic administration of exosomes released from mesenchymal stromal cells promote functional recovery and neurovascular plasticity after stroke in

rats. J. Cereb. Blood Flow Metab. *33*, 1711-1715.

Yang, H., Yang, H., Xie, Z., Wei, L., and Bi, J. (2013). Systemic transplantation of human umbilical cord derived mesenchymal stem cells-educated T regulatory cells improved the impaired cognition in AβPPswe/PS1dE9 transgenic mice. PLoS One *8*, e69129.

Zhang, X., Chen, J., Liu, A., Xu, X., Xue, M., Xu, J., Yang, Y., Qiu, H., and Guo, F. (2018). Stable overexpression of p130/E2F4 affects the multipotential abilities of bone-marrow-derived mesenchymal stem cells. J. Cell. Physiol. *233*, 9739-9749.

Zhang, Y., Huang, X., and Yuan, Y. (2017). MicroRNA-410 promotes chondrogenic differentiation of human bone marrow mesenchymal stem cells through down-regulating Wnt3a. Am. J. Transl. Res. *9*, 136-145.

Zhang, Z., Lin, J., Chu, J., Ma, Y., Zeng, S., and Luo, Q. (2008). Activation of caspase-3 noninvolved in the bystander effect of the herpes simplex virus thymidine kinase gene/ganciclovir (HSV-tk/GCV) system. J. Biomed. Opt. *13*, 031209.